IOSR Journal of Electrical and Electronics Engineering (IOSR-JEEE)
e-ISSN: 2278-1676,p-ISSN: 2320-3331, Volume 10, Issue 5 Ver. I (Sep – Oct. 2015), PP 21-29
www.iosrjournals.org

Diagnosis methods of stator short circuit faults of BLDC Motor Using Adaptive Neuro-fuzzy Inference (ANFIS) system and Wavelet

V.Jaya lakshmi[1], M.V.Ramesh[2]
[1,2](EEE Department, Prasad V. PotluriSiddhartha Institute of Technology, India)

Abstract: *the fault in a Brushless DC (BLDC) Motors can lead to excessive downtimes that can lead to huge losses in terms of maintenance and production. This paper discusses the diagnosis of stator winding faults, which is one of the common faults in a Brushless DC Motors. Several diagnostics techniques have been presented in the literature. Fault detection using traditional analytical methods are not always possible as this requires prior knowledge of the exact motor model. The motor models are also susceptible to inaccuracy due to parameter variations. This paper presents Adaptive Neuro-fuzzy Inference system (ANFIS) based, and wavelet based fault diagnosis methods to diagnoses the fault. The dynamic characteristics of the brushless DC motor is observed and analyzed using the developed MATLAB/ simulink model. Control system response parameter such as, recovery time is observed and compared for the above controllers. In order to validate the performance of the proposed controller under realistic working environment, simulation result has been obtained and analyzed for varying load and varying set speed conditions.*

Keywords: *ANFIS, Brushless dc motors, fault diagnosis, short circuit, wavelet.*

I. Introduction

Brush Less DC motors or electronically commutated motors are electric motors powered by direct current electricity and having electronically commutation systems, rather than mechanical commentators and brushes. A BLDC motor has rotating permanent magnets and a fixed armature. An electronic controller replaces the brush/ commutator assembly of brushed DC motor which continually switches the phase to windings to keep the motor turning. A BLDC motor has trapezoidal waveform back-EMF with 120 electrical- degree wide conducting period .The current is rectangular in shape. At any instant of time during operation, or during one conducting period which is 60 electrical degrees, two of the stator phases are excited as positive and negative terminal while the third phase floats. One of the main features of BLDC motor is that the Back-EMF signals provide information about the rotor position in order to generate commutations patterns and sequence. BLDC machines are being used, often in critical high performance applications. Fault diagnosis and condition monitoring of BLDC machines are assuming a new importance. Early detection of faults and asymmetries could allow preventive maintenance to be performed and provide sufficient time for controlled shutdown of the affected process, thereby reducing the costs of outage time and repairs.

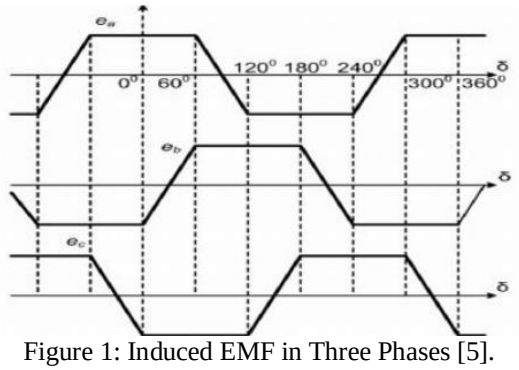

Figure 1: Induced EMF in Three Phases [5].

The range of faults that could occur in BLDC machines includes stator faults, rotor faults, and inverter faults. Yazici and Kliman [6] use short-time Fourier transforms (STFTs) and pattern-recognition techniques to detect faults in induction motors under varying operating conditions. Their application is however based on the assumption that the change in speed and load occurs very slowly and there are sufficiently long intervals of time wherein the motor can be assumed to operate in a stationary condition. This is common in

applications such as rolling steel mills and in the cement industry. Another approach to a similar application that uses wavelets is presented in [7].

II. Permanent Magnet Brushless Dc Motor

Permanent Magnet Brushless DC Motors (BLDC) is widely used in industrial applications. The BLDC motor usually consists of a stator with three phase armature windings and a rotor with permanent magnets. In BLDC motors, commutation is achieved by using power electronics coupled to feedback of rotor position from hall sensors. Compared with conventional brushed DC motors, the BLDC does not have a mechanical commutator which suffers from surface wear and electric arcing. The rare earth magnets on the rotor of the BLDC motor produce constant magnetic fields which lead to high efficiency and high power factor [1]. Particularly, the high torque-weight ratio of BLDC motors makes it very suitable for applications such as electric vehicles. The BLDC motors have many benefits over DC motors and induction motors,

- Better Speed Versus Torque Characteristics;
- High Dynamic Response;
- High Efficiency;
- Long Operating Life; And
- Noiseless Operation

BLDC motors can be categorized as surface mounted or interior mounted, according to the position and orientation of rotor permanent magnets [3]. In the case of the stator windings, BLDCs can be categorized as trapezoidal or sinusoidal, based on the shapes of their back-Electromotive-Force (back-EMF) waveforms. In addition to the back-EMF, the phase current also has corresponding trapezoidal or sinusoidal variations. The one with sinusoidal back EMF is also called Permanent Magnet Synchronous Motor (PMSM). For PMSM, the back-EMF generated in each phase winding by the rotation of the magnet is also sinusoidal.

In BLDCs, the magnetic fields generated in the stator and in the rotor are rotating synchronously. The stator of a BLDC motor consists of stacked steel laminations with windings kept in the slots that are axially cut along the inner periphery [2]. Most BLDCs have three stator star-connected windings [2].

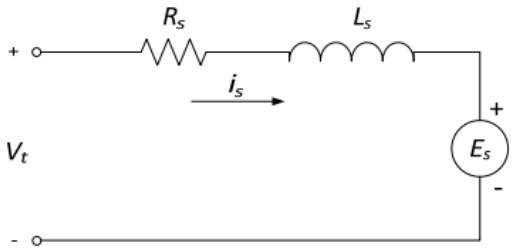

Figure.2.Simplified equivalent circuit of the BLDC motor.

In terms of modeling, a simplified equivalent circuit of one phase is given in Figure 2, where Vt is the voltage of the power supply, Rs is the resistance of the winding, Ls is the leakage inductance (Ls=L-M, where L is the self inductance of the winding and M is the mutual inductance), and Es is the back EMF induced in the winding by the rotating PM field.Based on the equivalent circuit, the performance of the BLDC motor can be described by the following equations [3]:

$$V_t = R_s I_s + L_s \frac{dI_s}{dt} + E_s \tag{1}$$

$$E_s = K_e \omega_r \tag{2}$$

$$T_e = K_T I_s \tag{3}$$

$$T_e = T_L + J\frac{d\omega_r}{dt} + K_{vis}\omega_r \tag{4}$$

where Ke is the back-EMF constant, ωr is the angular velocity of the rotor, KT is the torque constant, TL is the load torque, and Kvis is viscous friction coefficient.

III. Major Faults In Bldc Motors

Major Faults of BLDC Motors are Broken rotor bar, Static & dynamic air gap irregularities, Dynamic eccentricity, Winding short, Bearing & gearbox failure.

1**.** Inverter faults**:** BLDC motors are inverter fed. Many faults can occur in the inverter, such as the loss of one or more of the switches of a phase, the short circuit of a switch, and the opening of one of the lines to the machine.

2**.** Rotor faults: in BLDC machines are eccentricities, damaged rotor magnets, & damaged Hall sensors. All of these rotor faults cause problems such as vibration & noise.

3. Stator Faults:stator faults are breakdown of the winding insulation.This usually occurs in the region where the end windings enter the stator slots. It is caused by large electrical voltage stresses, electro dynamic forces produced by winding currents, thermal aging from multiple heating & cooling cycles, and mechanical vibrations from internal & external sources.

IV. Diagnostic Methods To Detect Faults

Diagnostic Methods to detect faults are Electromagnetic field monitoring, Temperature measurements, RF emission monitoring, Noise & vibration monitoring; Motor Current Signature Analysis (MCSA), AI & NN based techniques. The signal processing tools include DFT, FFT, STFT and Wavelet transform. Artificial intelligence is also used for fault diagnosis. These techniques include the applications of expert systems, genetic algorithm, neural networks and fuzzy logic. Modern techniques are based on application of advanced DSP tools on stator currents for fault diagnosis i.e. MCSA. Faults can be diagnosed using any one of signal processing techniques. These signal processing techniques cannot be used for diagnosing every type of faults.

1. Fault Diagnosis in BLDC Motors

- When the fault happens, the motor can be operated without breakdown, but it is necessary to maintain the motor for continuous working. Several methods have been applied to detect faults. It is important to be able to detect faults while they are still developing. This is called incipient failure detection. Timely warning that can be followed by maintenance can avoid catastrophic failures & costly long down times. The incipient detection of failures also results in a safer operating environment. Faults can occur either in stator, rotor, inverter or in the external systems connected to the motor.
- Vibration monitoring is the most popular choice for condition monitoring but it is preferred for use only in large machines where expensive accelerometers can be afforded.
- Electrical monitoring, which includes current based monitoring, is the most recent of all condition monitoring techniques and is inexpensive as electrical sensors are lower in cost compared to mechanical transducers.
- Condition monitoring is defined as the continuous evaluation of the health of the plant and equipment throughout its service life. It is used to detect various types of faults such as rotor fault, short winding fault, air gap eccentricity fault, bearing fault, load fault etc.
- Current monitoring does not require additional sensors because basic electrical quantities associated with electromechanical plants such as current & voltage are readily measured by tapping into existing voltage & current transformers that are always installed as part of protection system. It is non intrusive & implemented in motor control centre remotely from the motors being monitored.

2. Methods for Current Monitoring

- Methods for current monitoring are MCSA (Motor Current Signature Analysis) & Park Vector approach. MCSA uses the current spectrum of machine for locating characteristic fault frequencies. When a fault is present, the frequency spectrum of the line current becomes different from healthy motor. Such fault modulates air gap & produces rotating frequency harmonics in the self & mutual inductances of machine.

V. Adaptive Neuro-Fuzzy Inference System (Anfis)

The general ANFIS control structure contains the same components as the FIS except for the neural network block. The structure of the network is composed of set of units (and connections) arranged in five connected network layers, i.e., layer 1 to layer 5. The proposed ANFIS controller structure consists of four important blocks that are fuzzification, knowledge base, neural network and the Defuzzification. Layer 1 consists of input variables (membership functions) and triangular or bell shaped membership functions. Layer 2 is membership layer and it checks for the weights of each membership functions. It receives the input values from the first layer and act as membership functions to represent the fuzzy sets of the respective input variables. Layer 3 is called as rule layer and it receives input from the previous layer. Each node (each neuron) in this layer performs the pre-condition matching of the fuzzy rules. This layer computes the activation level of each rule and the number of layers equals to the number of fuzzy rules. Each node of this layer calculates the weights which will be normalized. Layer 4 is the defuzzification layer which provides the output values resulting from

the inference of rules. Layer 5 is called as the output layer which sums up all the inputs coming from layer 4 and transforms the fuzzy classification results into a crisp value. ANFIS modeled by Takagi–Sugeno (T–S) type systems are considered and it must have the following properties: It must be first or zero order T–S type system. It should have a single output, obtained using weighted average defuzzification. All output membership functions must be of the same type and it must be either linear or constant. It must have no rule sharing, i.e., different rules cannot share the same output membership function. The number of output membership functions must be equal to the number of rules. It must have unity weight for each rule. The ANFIS structure is tuned automatically by least-square estimation and the back propagation algorithm. Because of its flexibility, the ANFIS strategy can be used for a wide range of control applications.The algorithm presented above is used in the proceeding section to develop the ANFIS controller for controlling the speed of BLDC motor.

1. ANFIS control scheme for speed control of BLDC motor

The development of the control strategy for speed control of the BLDC motor with proposed ANFIS controller is presented in Fig. 3. It consists of two loops namely inner loop and outer loop. Inner loop is used for synchronizing the inverting gate signal with back electro motive force or rotor position of the motor. The outer loop is used for controlling the speed of the BLDC motor by controlling

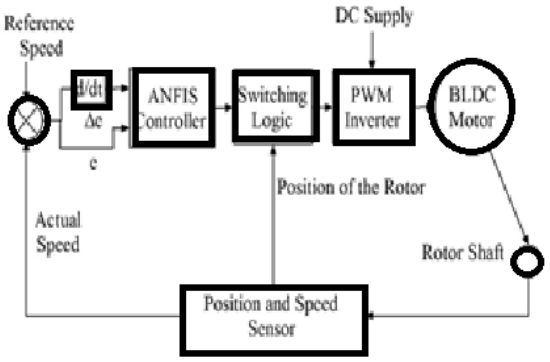

Fig. 3. Proposed ANFIS controller for BLDC motor.

The dc bus voltage through PWM inverter. Based upon error and rate of change of error, ANFIS controller provides the control signal to the switching logic circuit. The switching logic circuit provides the PWM signal for the inverter gate with respect to rotor position of the motor and the control signal output obtained from ANFIS controller. ANFIS incorporates artificial neural network with fuzzy inference system and first-order Takagi–Sugeno fuzzy model is used in this work. The analysis has two inputs, error (e), rate of change of error (Δe) and the output is control signal. The if–then rules are given in the following equation:

$$\begin{aligned}
&\text{Rule 1: IF } e \text{ is } A_1;\ \Delta e \text{ is } B_1;\ \text{then } f_1 = P_1^* e + R_1^* \Delta e + s_1\\
&\text{Rule 2: IF } e \text{ is } A_1;\ \Delta e \text{ is } B_2;\ \text{then } f_2 = P_2^* e + R_2^* \Delta e + s_2\\
&\vdots\\
&\text{Rule } i-1\text{: IF } e \text{ is } A_j;\ \Delta e \text{ is } B_{j-1};\ \text{then } f_{i-1} = P_{i-1}^* e + R_{i-1}^* \Delta e + s_{i-1}\\
&\text{Rule } i\text{: IF } e \text{ is } A_j;\ \Delta e \text{ is } B_j;\ \text{then } f_i = P_i^* e + R_i^* \Delta e + s_i
\end{aligned} \tag{5}$$

Where

$$e = \omega ref - \omega r \tag{6}$$

$$\Delta e = \frac{d(\omega_{ref} - \omega_r)}{dt} \tag{7}$$

$$f_i = P_i e + R_i \Delta e + s_i \tag{8}$$

where ωref is the reference speed, ωr is the actual rotor speed, j¼1, 2, …, q, i¼1, 2, …, q2, A and B are the fuzzy membership sets defined for input variables e and Δe. q is the number of membership functions for the fuzzy systems of inputs e and Δe. fi is the linear consequent functions defined in terms of inputs e and Δe. Pi, Ri and si are consequent parameters of an ANFIS fuzzy model. Same-layer nodes of an ANFIS model have similar functions. Output signals from the nodes of a preceding layer are the input signals to the next layer. The structure of five layer ANFIS is shown in Fig. 4. The error and rate of change of error, i.e., e and Δe as mentioned in Eqs. (6) and (7) are given as input to layer 1. In layer 1, every node is an adaptive node with a

particular fuzzy membership function specifying the degrees of the inputs which satisfies the quantifier. The following equation represents the node outputs for the two inputs:

$$L_{1,j} = \mu A_j(e) \quad \text{for } j = 1, 2, \ldots, q$$
$$L_{1,j} = \mu B_j(\Delta e) \quad \text{for } j = 1, 2, \ldots, q \tag{9}$$

The membership functions considered for A and B in Eq. (9) are triangular-shaped functions and their representations are given in

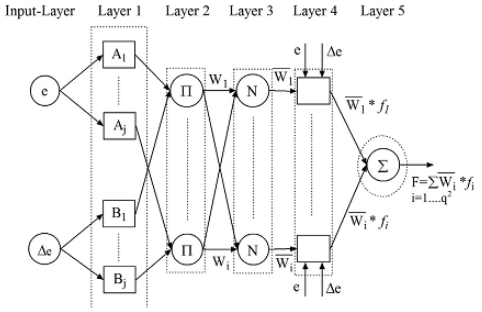

Fig. 4. Structure of a five-layer ANFIS.

The following equations:

$$\mu A_j(e, a_j, b_j, c_j) = \begin{cases} 0, & e \le 0 \\ \frac{e-a_j}{b_j-a_j}, & a_j \le e \le b_j \\ \frac{c_j-e}{c_j-b_j}, & b_j \le e \le c_j \\ 0, & c_j \le e \end{cases} \tag{10}$$

$$\mu B_j(\Delta e, x_j, y_j, z_j) = \begin{cases} 0, & \Delta e \le 0 \\ \frac{\Delta e-x_j}{y_j-x_j}, & x_j \le \Delta e \le y_j \\ \frac{z_j-\Delta e}{z_j-y_j}, & y_j \le \Delta e \le z_j \\ 0, & z_j \le \Delta e \end{cases} \tag{11}$$

The parameters for fuzzy membership functions are aj, bj, cj, xj, yj and zj. The triangular-shaped function changes its pattern with corresponding changes in the parameters. This change will provide various contours of the triangular-shaped function in accordance with the data set for the problem considered. Parameters in this layer are known as premise parameters. In layer 2, every node is a fixed node labeled π. L2,i output is the product of all incoming signals and it is given in the following equation:

$$L_{2,i} = W_i = \begin{bmatrix} W_1 & \cdots & W_q \\ \vdots & \ddots & \vdots \\ W_{q^2-(q-1)} & \cdots & W_{q^2} \end{bmatrix} = \begin{bmatrix} \mu A_1 \times \mu B_1 & \cdots & \mu A_1 \times \mu B_q \\ \vdots & \ddots & \vdots \\ \mu A_q \times \mu B_1 & \cdots & \mu A_q \times \mu B_q \end{bmatrix} \tag{12}$$

Each of the second layer's node output represents the firing strength of the associated rule. The T-norm operator algebraic product (TAB (A, B)¼A B) is used to obtain the firing strength (Wi). In layer 3, every node is a fixed node labeled N. The output of the ith node is the ratio of the firing strength of the ith rule (Wi) to the sum of the firing strength of all the rules and is given in the following equation:

$$L_{3,i} = \overline{W_i} = \frac{W_i}{\sum_{1=1}^{q^2} W_i} \tag{13}$$

This output gives a normalized firing strength. In layer 4, every node is an adaptive node with a node function given by the following equation:

$$L_{4,i} = \overline{W_i} f_i = \overline{W_i}(P_i e + R_i\ \Delta e + s_i) \tag{14}$$

Where Wi is the normalized firing strength from layer 4 and Pi, Ri, and si are the control signal parameter sets of this node. Parameters in this layer are known as consequent parameters. In layer5, the single node is a fixed node labeled Σ. It computes the overall output as the summation of all incoming signals and it is given in the following equation:

$$L_{5,1} = \sum_i \overline{W_i} f_i = \frac{\sum_i W_i f_i}{\sum_i W_i} \tag{15}$$

Next, the process of applying hybrid learning algorithm to identify ANFIS parameters has been discussed. For the learning process, the initial input membership function and number of rules for fuzzy inference system for the input–output training data sets should be specified. Basically, the number of membership function assigned to each input variable is chosen experimentally, i.e., by plotting the data sets and

examining them visually or simply by trial and error approach. For data sets with more than one input, visualization techniques are not very effective and one has to rely on trial and error approach.

VI. Wavelet

Wavelet may be seen as a complement to classical Fourier decomposition method.Suppose, a certain class of functions is given and we want to find 'simple functions' f0, f1, f3,..... such that each

$$f(x) = \sum_{n=0}^{\infty} a_n f_n(x)$$

For some coefficients an.Wavelet is a mathematical tool leading to representations of the type (1) for a large class of functions f.Wavelet theory is very new (about 25 years old) but has already proved useful in many contexts.

1. Definition (Wavelet)

A wavelet means a small wave (the sinusoids used in Fourier analysis are big waves) and in brief, a wavelet is an oscillation that decays quickly. Equivalent mathematical conditions for wavelet are:

$$\int_{-\infty}^{\infty} |\psi(t)|^2 \, dt < \infty$$

$$\int_{-\infty}^{\infty} \frac{|\hat{\psi}(\omega)|^2}{|\omega|} d\omega < \infty$$

$$\int_{-\infty}^{\infty} |\psi(t)| dt = 0$$

Where $(\psi)(\omega)$ is the Fourier Transform of $\psi(t)$. Equation (4) is called the admissibility condition.

2. Wavelet Transform

Jean Morlet in 1982 introduced the idea of the wavelet transform and provided a new mathematical tool for seismic wave analysis. Morlet first considered wavelets as a family of functions constructed from translations and dilations of a single function called the "mother wavelet" $\psi(t)$. They are defined by

$$\psi_{a,b}(t) = \frac{1}{\sqrt{|a|}} \psi\left(\frac{t-b}{a}\right), \qquad a,b \in \mathbb{R},\ a \neq 0$$

The parameter a is the scaling parameter or scale, and it measures the degree of compression. The parameter b is the translation parameter which determines the time location of the wavelet. If $|a| < 1$, then the wavelet in (5) is the compressed version (smaller support in time- domain) of the mother wavelet and corresponds mainly to higher frequencies. On the other hand, when $|a| > 1$, then $\psi a,b(t)$ has a larger time-width than $\psi(t)$ and corresponds to lower frequencies. Thus, wavelets have time-widths adapted to their frequencies. This is the main reason for the success of the Morlet wavelets in signal processing and time-frequency signal analysis.

3. Wavelet Series and Wavelet Coefficients

If a function $f \in L2(R)$, the series

$$\sum_{j \in z} \sum_{k \in Z} \langle f, \psi_{j,k} \rangle \, \psi_{j,k}(t)$$

Is called the wavelet series of f and

$$\langle f, \psi_{j,k} \rangle = d_{j,k} = \int_{-\infty}^{\infty} f(t) \psi_{j,k}(t) dt$$

is called the wavelet coefficients of f .

4. Signal

A signal is given as a function f which has a series representation

$$f(x) = \sum_{n=0}^{\infty} a_n x^n$$

Then all information about the function f is stored in the coefficients $\{an\}^{\infty}n=0$.

5. Classification of Signals

We can split the class of signals into two classes, namely:

1. Continuous signals

2. Discrete signals

Continuous Signals**:**The signals which is described by a continuous function (for example a recording of a speech signal or music signal, which measures the current in the cable to the loudspeaker as a function of time) is called continuous signals Christensen [13], Mallat [14].

Discrete Signals:The signal which is described by a sequence of numbers or pairs of numbers is called discrete signals Christensen [13], Mallat [14]. Here mentioned one example of discrete signals:

An Example

A digital black-white photo consists of a splitting of the picture into a large number of small squares, called pixels; to each pixel, the camera associates a light intensity, measured on a scale from, say, 0 (completely white) to 256 (completely black). Put together, this information constitutes the picture. Thus, mathematically a photo consists of a sequence of pairs of numbers, namely, a numbering of the pixels together with the associated light intensity Christensen [13], Mallat [14].

VII. Block Diagram And Simulation Results

The 3-Ø Ac output voltage of the inverter is applied to stator windings of the PMSM.The inverter gates signals are created by decoding the Hall Effect signals of the motor. The Load Torque applied to the shaft of machine from 0 to its nominal value in steps.The gate signals are developed according to the hall sensor signals, stator currents are given to protection using ANFIS and wavelets block and this block produces the gate signals according to the logic written in that block.

This scheme is simulated in SIMULINK/MATLAB.When stator currents exceed the normal full load value, the adaptive nuero fuzzy control(ANFIS),wavelets are used to decompose the stator currents increases. The motor gets paused when this value greater than the value specified in the program.

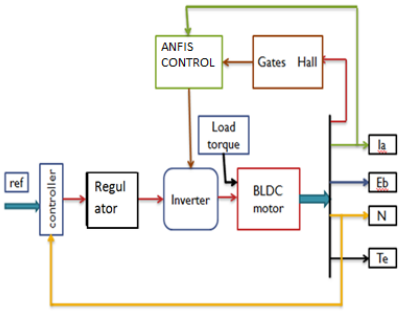

Fig:3

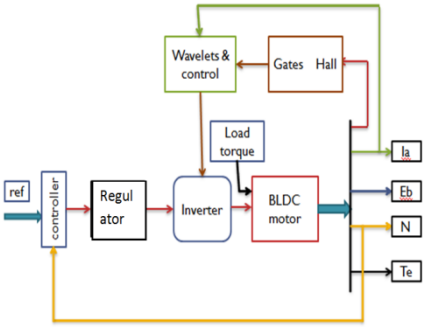

fig:4

Figure3 and figure4 shows the block diagram of stator short circuit protection scheme for PMBLDCM using ANFIS and using wavelet respectively.

The following figures Fig.5.Fig.6. fig.7. Shows The Output Wave Form Of Stator Current, Electromotive Force,Electromagnetic Torque and rotor speed waveforms With Three Phase BLDC Motor Drive without Stator Fault.

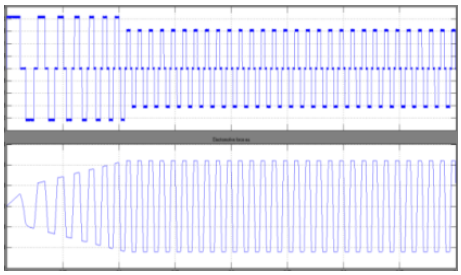

Fig.5.Stator current and electromotive force.

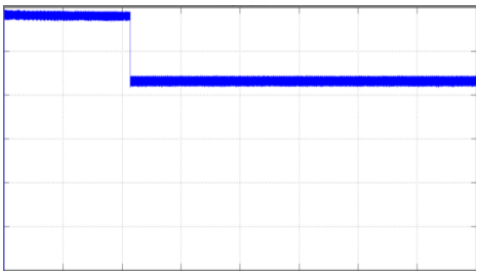

Fig.6.Electromagnetic Torque.

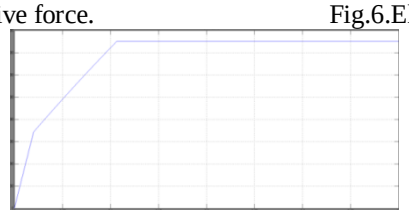

Fig.7.Rotor speed.

The following figures Fig.8. Fig.9. Shows The Output Wave Form Of Stator Current, Electromotive Force, Electromagnetic Torque and rotor speed With Three Phase BLDC Motor Drive with Stator Fault.

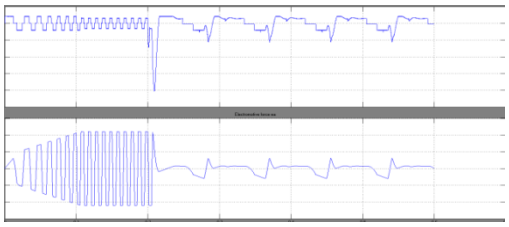

Fig:8 Stator current and electromotive force

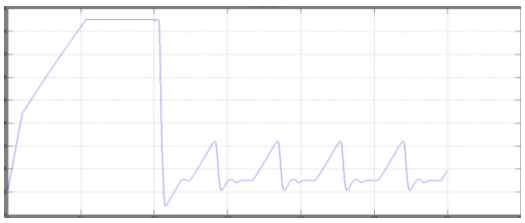

fig:9 Electromagnetic Torque

The following figures Fig10,fig11,fig12 shows the output wave form of Stator Current and Electromotive Force and Rotor Speed with wavelet protection.

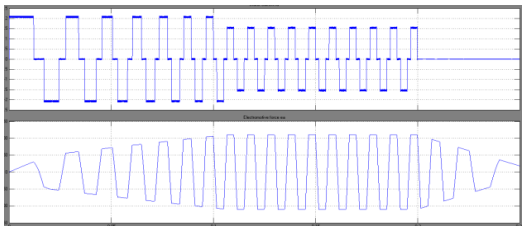

Fig.10stator current and electromotive force

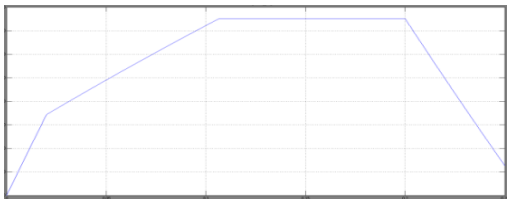

Fig.11.rotor speed.

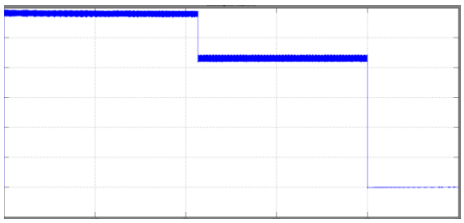

Fig.12.Electromagnetic torque.

The following figures Fig13,fig14,fig15 shows the output wave form of Stator Current and Electromotive Force and Rotor Speed with ANFIS control scheme.

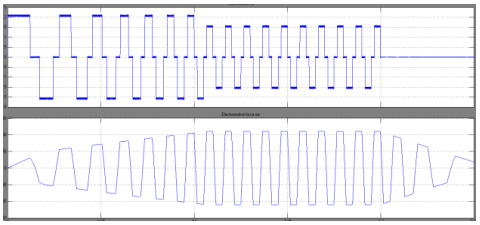

Fig.13stator current and electromotive force

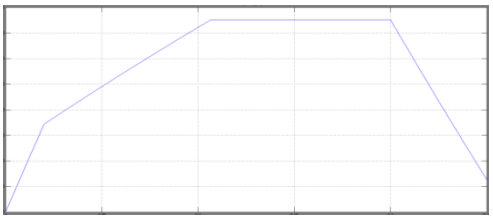

Fig.14.rotor speed.

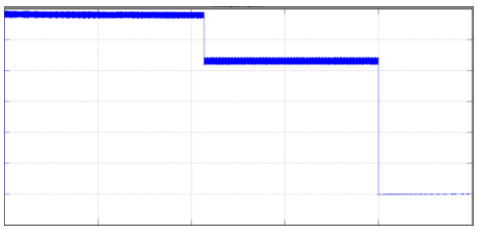

Fig.15.Electromagnetic torque.

VIII. Conclusion

Fault current develops a braking torque component that tends to reduce the average torque of the machine. Operation with net negative torque (totally braking) is possible, especially under large number of shorted turns with high-speed, low-torque conditions. Current command should increase during the fault in order to obtain the same normal operation torques. Also, time periods of full-load operation should be minimized to avoid the excessive heat loss associated with the fault.

This paper presets the two independent schemes for automatic fault diagnosis of stator faults of BLDCM. Approximation and detail coefficients of obtained stator currents and are calculated by using discrete wavelets. When the maximum of the approximation value exceeds the specified value than the PMDCM gets stopped. .

The diagnostic process is automated through ANFIS-based agents. ANFIS training and testing are completed off line based on indices derived from simulated waveforms. compared to wavelet method ANFIS gives fast and accurate results.

References

[1] J. Penman, H. G. Sedding, B. A. Lloyd, and W. T. Fink, "Detection and location of inter turn short circuits in the stator windings of operating motors," IEEE Trans. Energy Convers., vol. 9, no. 4, pp. 652–658, Dec. 1994.

[2] A. Stavrou, H. G. Sedding, and J. Penman, "Current monitoring for detecting inter-turn short circuits in induction motors," IEEE Trans. Energy Convers., vol. 16, no. 1, pp. 32–37, Mar. 2001.

[3] G. M. Joksimovic and J. Penman, "The detection of inter-turn short circuits in the stator windings of operating motors," IEEE Trans. Ind. Electron., vol. 47, no. 5, pp. 1078–1084, Oct. 2000.

[4] R. M. Tallam, T. G. Habetler, R. G. Harley, D. J. Gritter, and B. H. Burton, "Neural network based on-line stator winding turn fault detection for induction motors," in Proc. IEEE-Industry Applications Soc. Conf., vol. 1, 2000, pp. 375–380.

[5] R. M. Tallam, T. G. Habetler, and R. G. Harley, "Stator winding turn fault detection for closed-loop induction motor drives," IEEE Trans. Ind. Appl., vol. 39, no. 3, pp. 720–724, May/Jun. 2003.

[6] A. J. M. Cardoso, S. A. M. Cruz, and D. S. B. Fonseca, "Inter-turn stator winding fault diagnosis in three-phase motors, by Park's vector approach," IEEE Trans. Energy Convers., vol. 14, no. 3, pp. 595–598, Sep. 1999.

[7] M. E. H. Benbouzid and G. B. Kliman, "What stator current processing based technique to use for induction motor rotor faults diagnosis?," IEEE Trans. Energy Convers., vol. 18, no. 2, pp. 238–244, Jun. 2003.

[8] M. A. Awadallah and M. M. Morcos, "Application of AI tools in fault diagnosis of electrical machines and drives—an overview," IEEE Trans. Energy Convers., vol. 18, no. 2, pp. 245–251, Jun. 2003.

[9] F. Filippetti, G. Franceschini, C. Tassoni, and P. Vas, "Recent developments of induction motor drives fault diagnosis using AI techniques," IEEE Trans. Ind. Electron., vol. 47, no. 5, pp. 994–1004, Oct. 2000.

[10] J.-S. R. Jang, "ANFIS: adaptive-network-based fuzzy inference system," IEEE Trans. Syst., Man, Cybern., vol. 23, no. 3, pp. 665–685, May/Jun. 1993.

[11] S. Altug, M.-Y. Chow, and H. J. Trussel, "Fuzzy inference systems implemented on neural architectures for motor fault detection and diagnosis," IEEE Trans. Ind. Electron., vol. 46, no. 6, pp. 1069–1079, Dec. 1999.

[12] N. A. Demerdash and T. W. Nehl, "Dynamic modeling of brushless DC motors for aerospace actuation," IEEE Trans. Aerosp. Electron. Syst., vol. 16, no. 6, pp. 811–821, Nov. 1980.

[13]. Christensen, O. Approximation Theory, From Taylor Polynomials to Wavelets. Birkhäuser, Boston, 2004.

[14]. Mallat, S. A wavelet Tour of Signal Processing. Academi Press, New York, 1999.

Jaya lakshmi received the B. Tech degree in Electrical and Electronics Engineering from potti sri ramulu college of Engineering and technology College in 2013 and pursuing M.Tech in Power System Control and Automation at Prasad V. Potluri Siddhartha Institute of Technology. Her research includes Electrical Machines and Power System Operation and Control.

M.V.Ramesh received the B.Tech degree in Electrical and Electronics Engineering from Nagarjuna University in the year 1998 and M.S (Electrical Engineering) from German University in the year 2002. He is working as an Associate Professor at P.V.P.S.I.T, Vijayawada and recently received the doctorate. His research interests include Power Electronics and Drives, Power System Automation, Hybrid Vehicle Design and Reactive Power Compensation. He published several papers at the national and international journals and conferences.